Hindawi
Shock and Vibration
Volume 2019, Article ID 1475981, 13 pages
https://doi.org/10.1155/2019/1475981

Research Article

Instantaneous Modal Parameter Identification of Linear Time-Varying Systems Based on Chirplet Adaptive Decomposition

Jie Zhang and Zhiyu Shi

State Key Laboratory of Mechanics and Control of Mechanical Structures, Nanjing University of Aeronautics and Astronautics, Nanjing 210016, China

Correspondence should be addressed to Zhiyu Shi; zyshi@nuaa.edu.cn

Received 15 August 2019; Revised 22 November 2019; Accepted 2 December 2019; Published 28 December 2019

Academic Editor: Roger Serra

Instantaneous modal parameter identification of time-varying dynamic systems is a useful but challenging task, especially in the identification of damping ratio. This paper presents a method for modal parameter identification of linear time-varying systems by combining adaptive time-frequency decomposition and signal energy analysis. In this framework, the adaptive linear chirplet transform is applied in time-frequency analysis of acceleration response for its higher energy concentration, and the response of each mode can be adaptively decomposed via an adaptive Kalman filter. Then, the damping ratio of the time-varying systems is identified based on energy analysis of component response signal. The proposed method can not only improve the accuracy of instantaneous frequency extraction but also ensure the antinoise ability in identifying the damping ratio. The efficiency of the method is first verified through a numerical simulation of a three-degree-of-freedom time-varying structure. Then, the method is demonstrated by comparing with the traditional wavelet and time-domain peak method. The identified results illustrate that the proposed method can obtain more accurate modal parameters in low signal-to-noise ratio (SNR) scenarios.

1. Introduction

System identification techniques have received significant attention in civil, aerospace, and mechanical engineering in the past few decades [1]. Most of them assume that the analyzed systems are linear time-invariant (LTI), i.e., the output for such systems does not change with a delay in the input. However, in reality, this assumption is not valid for many engineering structures which are damaged or subjected to strong excitation. Thus conventional modal analysis methods and experimental techniques are not appropriate for these linear time-varying (LTV) systems [2]. In such cases, for the purpose of health monitoring or damage identification, it is necessary to develop reliable approaches for the identification of time-varying characteristics.

In terms of LTV system identification, many methods have been developed for various time-varying cases. These methods generally belong to two categories: time-domain methods and time-frequency-domain methods [3].

In the time domain, identification methods based on the time-varying model such as state-space model and time series model have become the main research objects since the time-domain description of LTV systems is very convenient. Liu [4] proposed a subspace-based identification technique and used eigenvalues of the estimated transition matrices to characterize the dynamic properties. The subspace is constructed by the singular value decomposition (SVD) which costs too much computational time. Authors in [5–7] further presented improved algorithm to overcome such drawback. Pang et al. [7] utilized the projection approximation subspace tracking (PAST) technique instead of the SVD. Zhou et al. [8] presented a postprocess method to improve the quality of identification results in low signal-to-noise ratio scenarios. Meanwhile, parameter identification is established based on the autoregressive-moving-average

(ARMA) model which can match the structures of real-world processes. In order to process nonstationary signals and identify the parameters of time-varying structures, many approaches were also proposed based on the time-dependent autoregressive moving average (TARMA) model [9]. The TARMA model can be utilized as an efficient tool to reveal the dynamic characteristics of nonstationary signals due to its simplicity and effectiveness. However, a continuing challenge is how to establish a precise TARMA model. Typically, the recursive least-squares (RLS) approach and the Kalman filter [10] were applied to solve the problem. Recently, Spiridonakos and Fassois [11] presented an adaptable functional series TARMA model for nonstationary signal modelling, which employs the B-spline function to model the TARMA coefficients adaptively and structurally. Yang et al. [12] developed a moving Kriging shape function modelling of vector TARMA models, which has the advantage on the sudden change.

Furthermore, time-frequency (TF) estimators have been more extensively studied, i.e., by using the Hilbert transform (HT) and wavelet transform (WT), since the response of LTV systems is a typical nonstationary signal which needs to be processed by time-frequency analysis (TFA) tools. Meanwhile, TFA tools become effective in solving time-varying equations with the development of TF theory. Shi et al. [13] firstly addressed the Hilbert transform and empirical mode decomposition (EMD) method to identify time-varying multi-degree-of-freedom (MDOF) systems. Ghanem and Romeo [14] presented a wavelet-based identification method, which projects the governing differential equation on a subspace spanned by a finite number of wavelets and identifies the parameters using the Galerkin approach. Furthermore, a wavelet-based state-space method for LTV system identification was proposed by Xu et al. [15]. Hou et al. [16, 17] proposed a continuous wavelet-based technique for identification of instantaneous modal parameters of time-varying structures. Dziedziech et al. [18] used the wavelet-based frequency response function (FRF) for modal identification of time-variant systems. An identification approach based on the empirical wavelet transform (EWT) was developed for LTV systems by Xin et al. [19].

As seen from the above analysis, conventional TFA methods are suitable for processing such nonstationary signals of LTV systems. However, they are insufficient to provide a TF representation with high resolution due to their inherent restrictions. HT can process multicomponent signals only when combined with EMD which always has the shortage of modal aliasing and end swing phenomena. For short-time TFA tools like WT [20, 21], they are established on the assumption of the considered signal being piecewise stationary in a short time. This means that they essentially use horizontal lines to approximate the IF feature. To improve the performance of the TFA methods, many effective methods have been proposed. One relatively effective strategy named synchrosqueezing transform (SST) [22] is to squeeze the TF coefficients into the instantaneous frequency trajectory. However, the strongly modulated frequency component and noise could destroy the original TF representation of the signal heavily. Another strategy named parameterized TFA was inspired by the fact that using adaptive window function (such as adding chirp rate in base function) in WT can achieve a much higher TF resolution. Thus the chirplet transform (CT) was designed by Deng et al. [23]. By using an extra parameter, chirp rate, the CT is able to create a concentrated TF representation for the linear modulated signal. In order to search the best chirp rate according to the TF signature of nonstationary signal, Yu and Zhou [24] developed an adaptive algorithm named GLCT. In terms of the TF characteristics of vibration response, the responses of LTV systems are usually characterized by multicomponent amplitude-modulation (AM) and frequency-modulation (FM) signals. Therefore, the CT is particularly suitable for identifying the instantaneous frequency of time-varying signals. In addition, for nonstationary signals with noise, the Vold–Kalman (VK) filter can more effectively decompose the multicomponent signals [25] compared with EMD.

This paper presents a time-frequency decomposition method to extract the individual modes from the free response signal of LTV systems. The IF is extracted based on GLCT as the complex carrier wave of the signal, and then, the VK filter is constructed to perform signal decomposition adaptively. Using this method, the IF of each time-varying component can be identified more accurately, and the amplitude envelope of each signal component can be also obtained. Thus many damping ratio identification methods based on amplitude envelope were proposed such as the time-domain method [26, 27]. The identification of damping ratio is of great value for many engineering applications such as flutter analysis of aircraft. But this task is of challenges since the amplitude envelope is easily disturbed by noise which leads to a much lower identification accuracy of damping ratio than frequency. Considering this shortcoming, the improvement based on energy analysis [28] is explored to make the identification method insensitive to noise. The damping ratio is identified by energy ratio of adjacent half-periodic signals, which can effectively eliminate the effect of noise on amplitude. The aim of this paper is to improve the identification accuracy of instantaneous modal parameters, i.e., instantaneous frequencies and damping ratios.

With this prime objective, this paper is organized as follows: the theory of time-frequency decomposition based on GLCT and VK filter is briefly introduced in Section 2. The energy analysis for damping ratio identification of LTV systems is presented in Section 3. Section 4 shows a series of comparative numerical simulation examples to illustrate the performance of identification. In these comparative examples, the Morlet wavelet and time-domain peak method are selected for comparison to identify instantaneous frequencies and damping ratios, respectively. Finally, Section 5 provides the discussion and conclusions on the identification results.

2. Theoretical Background

Using the adaptive TF method for vibration signal decomposition consists of two main steps: (1) performing TFA

of the target vibration signals by using GLCT to extract the TF ridge of each time-varying component and (2) constructing the filtering band based on the extracted TF ridge, then decomposing the target vibration signals into multicomponent AM and FM signals to obtain the amplitude envelope. To apply this TF method for LTV systems, we can identify the instantaneous frequencies based on the TF ridge and identify the damping ratio based on the amplitude envelope, respectively.

2.1. General Linear Chirplet Transform (GLCT). GLCT is an approach to obtain the best demodulated operator for signals with time-varying IF, which has better performance than any individual CT in generating TF representation.

According to the theory of Ville, an analytic signal with time-varying IF can be written as

$$s(t) = a(t)e^{j\int \varphi(t)\mathrm{d}t}, \tag{1}$$

where $a(t)$ is the amplitude and $\varphi(t)$ is the IF of the signal.

In a short time τ, $\varphi(t)$ can be regarded as a linear equation approximately, which can be expanded by the Taylor expansion:

$$\varphi(\tau) = \varphi(t) + \varphi'(t)(\tau - t), \tag{2}$$

where $\varphi(t)$ is the IF at time t and $\varphi'(t)$ is the first-order derivative of IF at time t.

The CT of signal $s(t)$ which considers the time-variant demodulated operator can be written as

$$\mathrm{CT}(t, \omega, c(t)) = \int_{-\infty}^{+\infty} s(\tau) \cdot w(\tau - t) \cdot e^{-j\omega\tau} \cdot e^{-\left(jc(t)(\tau-t)^2\right)/2}\mathrm{d}\tau, \tag{3}$$

where $w(\tau - t)$ is a window function and $e^{-jc(t)(\tau-t)^2/2}$ is the time-variant demodulated operator.

The CT amplitude in IF $\varphi(t)$ ($\omega = \varphi(t)$) can be calculated by

$$\begin{aligned}
|\mathrm{CT}(t, \omega, c(t))| &= \left|\int_{-\infty}^{+\infty} w(\tau - t) \cdot a(\tau) \cdot e^{\left(j\varphi(\tau)\tau + j\varphi'(t)(\tau-t)^2\right)/2} \cdot e^{-j\varphi(t)\tau} \cdot e^{-jc(t)(\tau-t)^2/2}\mathrm{d}\tau\right| \\
&= \left|\int_{-\infty}^{+\infty} e^{j\left(\varphi'(t) - c(t)\right)(\tau-t)^2/2} \cdot w(\tau - t) \cdot a(\tau) \cdot \mathrm{d}\tau\right| \\
&\le \left|\int_{-\infty}^{+\infty} w(\tau - t)a(\tau)\mathrm{d}\tau\right|.
\end{aligned} \tag{4}$$

From equation (4), it can be seen that, when $c(t)$ in CT is consistent with $\varphi'(t)$ of the analyzed signal, the CT amplitude will achieve the maximum, and then the better TF representation with high energy concentration will be obtained. But for multicomponent signals, the IF feature cannot be known in advance, which leads to that it is hard to determine the demodulated operator accurately.

A feasible solution is to use a series of discrete demodulated operators to approximate the best demodulated operator [24]. Actually the demodulated operator is also a rotating operator of signals on the TF result, and the rotating degree is $\arctan(-c)$. So a parameter α is introduced to characterize the parameter c as

$$\alpha = \arctan\left|\frac{2T_s}{F_s}c\right|, \quad \alpha \in \left(-\frac{\pi}{2}, -\frac{\pi}{2}\right), \tag{5}$$

where T_s is the sampling time and F_s is the sampling frequency.

In a discrete way, the parameter α is divided into N_α values on the TF plane from $-(\pi/2)$ to $\pi/2$ as

$$\alpha = -\frac{\pi}{2} + \frac{\pi}{N_\alpha + 1}, \; -\frac{\pi}{2} + \frac{2\pi}{N_\alpha + 1}, \ldots, -\frac{\pi}{2} + \frac{N_\alpha\pi}{N_\alpha + 1}. \tag{6}$$

Then, equation (3) can be rewritten as

$$\begin{aligned}
\mathrm{CT}(t, \omega, c(t)) = \int_{-\infty}^{+\infty} & s(\tau) \cdot w(\tau - t) \cdot e^{-j\omega\tau} \\
& \cdot e^{-\left(\left(j\tan(\alpha)\left(F_s/2T_s\right)(\tau-t)^2\right)/2\right)}\mathrm{d}\tau.
\end{aligned} \tag{7}$$

From this, the TF spectrum with high energy concentration can be defined as

$$\mathrm{GSpec}(t, \omega) = \left|\mathrm{CT}\left(t, \omega, c_m\right)\right|^2, \tag{8}$$

where c_m is a discrete value when the CT amplitude achieves the maximum in TF point (t, ω), which can be calculated by

$$c_m = \arg\max|\mathrm{CT}(t, \omega, c(t))|. \tag{9}$$

In order to demonstrate the better TF representation of GLCT, WT and GLCT are used for TF analysis of a time-varying signal, respectively. The results are shown in Figure 1. It is shown that GLCT can adaptively track the instantaneous frequency trajectory at different TF points. Compared with WT, GLCT uses adaptive window function instead of rectangular TF window to achieve a much higher TF resolution. Thus, this approach can more adaptively and accurately estimate IF than traditional TFA tools especially for signals with time-varying IF.

2.2. Vold–Kalman Filter. In terms of nonstationary signal decomposition, various interesting approaches have been developed such as EMD [13], empirical wavelet transform

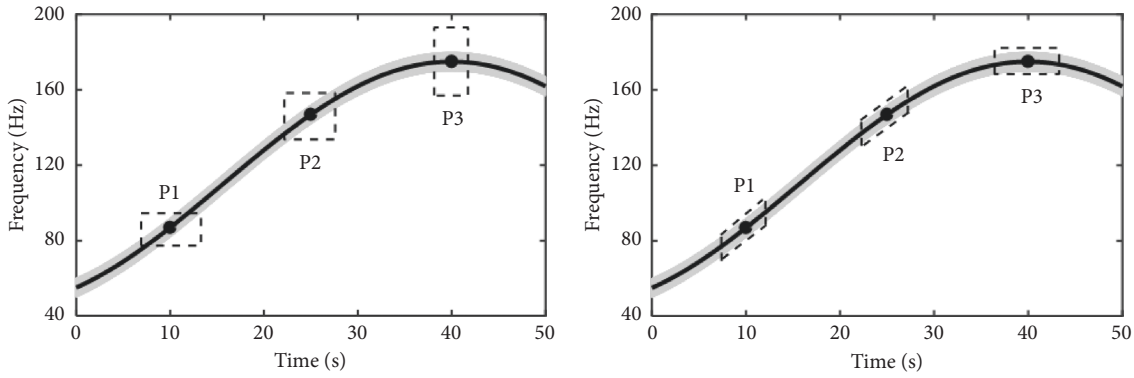

Figure 1: TF representation for a time-varying signal: (a) using WT and (b) using GLCT.

(EWT) [19], and Kalman filter [29]. But considering a multicomponent signal with time-varying IF in low SNR scenarios, the VK filter is more adapted for decomposing this signal [30]. Since the VK filter needs an estimation of the IF firstly, a novel time-frequency decomposition method is presented when GLCT is applied for IF extraction. In this section, the decomposition process is expounded in detail.

Consider a multicomponent analytic signal composed of component signal in equation (1) with random noise which can be written as

$$\begin{aligned} s(t) &= \sum_{k\in i} a_k(t)\Phi_k(t) + \mu(t) \\ &= \sum_{k\in i} a_k(t) e^{j\int \varphi_k(t)\mathrm{d}t} + \mu(t) \qquad (10) \\ &\qquad i = 1, 2, \ldots, K, \end{aligned}$$

where K is the number of component signals and $\mu(t)$ is a zero mean white noise.

In a discrete way, the signal is rewritten as

$$s(n) = \sum_{k\in i} a_k(n)\Phi_k(n) + \mu(n), \quad i = 1, 2, \ldots, K, \qquad (11)$$

where $n = 1, 2, \ldots, N$ and N is the total number of sampling points.

By using GLCT in TFA of this multicomponent signal, the IF of each component can be estimated. Thus, the complex-valued carrier wave $\Phi_k(n)$ can be constructed.

2.2.1. Structural Equation. It is assumed that the amplitude envelope $a_k(t)$ is the low-frequency modulation of the complex carrier wave $\Phi_k(t)$. In other words, envelope is locally approximated by a low-order polynomial, and it is filtered in some specific way. This condition can be expressed by a structural equation with the nonhomogeneity term $\varepsilon_k(n)$. The polynomial order designates the number of the filter poles. The equations for l-pole filter are given by

$$\nabla^l a_k(n) = \varepsilon_k(n). \qquad (12)$$

Taking $l = 2$ as an example, the corresponding equation is given by

$$\nabla^2 a_k(n) = a_k(n-1) - 2a_k(n) + a_k(n+1) = \varepsilon_k(n). \qquad (13)$$

The system of the structural equations containing all the samples takes the following form, which can be rewritten in the matrix form:

$$\begin{bmatrix} -2 & 1 & 0 & \cdots & 0 & 0 \\ 1 & -2 & 1 & \cdots & 0 & 0 \\ 0 & 1 & -2 & \cdots & 0 & 0 \\ \vdots & \vdots & \vdots & \ddots & \vdots & \vdots \\ 0 & 0 & 0 & \cdots & 1 & -2 \end{bmatrix} \begin{bmatrix} a_k(1) \\ a_k(2) \\ a_k(3) \\ \vdots \\ a_k(N) \end{bmatrix} = \begin{bmatrix} \varepsilon_k(1) \\ \varepsilon_k(2) \\ \varepsilon_k(3) \\ \vdots \\ \varepsilon_k(N) \end{bmatrix}, \qquad (14)$$

$$\mathbf{G}\mathbf{A}_k = \boldsymbol{\varepsilon}. \qquad (15)$$

2.2.2. Data Equation. Taking the measurement noise into account, the measurement equation is written in the matrix form:

$$\mathbf{S} - \begin{bmatrix} \mathbf{W}_1 & \mathbf{W}_2 & \mathbf{W}_3 & \cdots & \mathbf{W}_K \end{bmatrix} \begin{bmatrix} \mathbf{A}_1 \\ \mathbf{A}_2 \\ \mathbf{A}_3 \\ \vdots \\ \mathbf{A}_K \end{bmatrix} = \mathbf{U}, \qquad (16)$$

where $\mathbf{S} = \begin{bmatrix} s(1) \\ s(2) \\ s(3) \\ \vdots \\ s(N) \end{bmatrix}$, $\mathbf{W}_k = \begin{bmatrix} \Phi_k(1) & 0 & \cdots & 0 \\ 0 & \Phi_k(2) & \cdots & 0 \\ \vdots & \vdots & \ddots & \vdots \\ 0 & 0 & \cdots & \Phi_k(N) \end{bmatrix}$,

$\mathbf{A}_k = \begin{bmatrix} a_k(1) \\ a_k(2) \\ \vdots \\ a_k(N) \end{bmatrix}$, $\mathbf{U} = \begin{bmatrix} \mu(1) \\ \mu(2) \\ \mu(3) \\ \vdots \\ \mu(N) \end{bmatrix}$, and N is the number of sampling points.

2.2.3. Global Solution. The system of equations (15) and (16) is an underdetermined system for the unknown amplitude

envelope $a_k(t)$. The additional condition for the equation solution is that the variances of the nonhomogeneity terms $\varepsilon_k(n)$ and noise $\mu(n)$ have to be minimal while maintaining the given relationship between them.

The weighted sum of equations (15) and (16) gives the loss function:

$$J = \sum_{k\in i} r^2 \boldsymbol{\varepsilon}^T \boldsymbol{\varepsilon} + \mathbf{U}^T \mathbf{U} = \sum_{k\in i} r^2 \mathbf{A}_k^H \mathbf{G}^T \mathbf{G} \mathbf{A}_k + \left(\mathbf{S}^T - \sum_{k\in i} \mathbf{A}_k^H \mathbf{W}_k^H \right) \left(\mathbf{S} - \sum_{k\in i} \mathbf{W}_k \mathbf{A}_k \right), \tag{17}$$

where r is a weighting factor. The choice of a large value for the weighting factor r leads to the highly selective filtration in the frequency domain. In contrast, fast convergence with low-frequency resolution is achieved by choosing the small r value. The limit value of r [30] is shown in Table 1.

The first derivative of equation (17) with respect to the vector $\mathbf{A}_k$ gives a condition for the minimum of this function, which is called a normal equation:

$$\frac{\partial J}{\partial \mathbf{A}_k^H} = 0. \tag{18}$$

Thus the unknown envelope $\mathbf{A}_k$ results from equation (18).

3. Instantaneous Modal Parameter Identification of Linear Time-Varying Systems

3.1. Modal Response of Time-Varying Structures. The motion equation of a P-DOF LTV structure is given as

$$\mathbf{M}(t)\ddot{\mathbf{x}}(t) + \mathbf{C}(t)\dot{\mathbf{x}}(t) + \mathbf{K}(t)\mathbf{x}(t) = \mathbf{f}(t), \tag{19}$$

where $\mathbf{M}(t)$, $\mathbf{C}(t)$, and $\mathbf{K}(t)$ are time-varying mass, damping, and stiffness matrices, respectively; $\mathbf{x}(t)$ is the displacement response vector, $\dot{\mathbf{x}}(t)$ and $\ddot{\mathbf{x}}(t)$ are the velocity and acceleration response vectors, respectively; and $\mathbf{f}(t)$ is the excitation force vector on the structure.

Structural acceleration responses can be obtained as the superposition of P vibration modal responses [31], and when an impulse force is applied on the p-th dof, the acceleration response of the k-th generalized modal coordinate is given as

$$\ddot{x}_p(t) = \sum_{k=1}^{P} A_{0k} e^{-\xi_k(t)\omega_{0k}(t)t} \cos\left(\omega_{\mathrm{d}k}(t)t + \varphi_{0k}\right) = \sum_{k=1}^{P} \ddot{x}_{pk}(t) = \sum_{k=1}^{P} A_k(t)\cos\left(\varphi_k(t)\right), \tag{20}$$

where $\omega_{\mathrm{d}k}(t) = \omega_{0k}(t)\sqrt{1-\xi_k^2(t)}$ and $\xi_k(\mathrm{t})$, $\omega_{0k}(t)$, and $\omega_{\mathrm{d}k}(t)$ denote the k-th modal damping ratio, modal frequency, and natural frequency, respectively. It can be further written as the superposition of multicomponent AM-FM signals.

The acceleration impulse response signal of the time-varying structure is similar to multicomponent harmonic signals of equation (10). It can be adaptively decomposed by using the TF decomposition method proposed in this paper, thereby reconstructing each component signal, i.e., $A_k(t)\cos(\varphi_k(t))$.

Table 1: The value of the weighting factor.

Pole number	$s=1$	$s=2$	$s=3$	$s=4$
The max value of r	7×10^6	4×10^6	2×10^6	1.1×10^6

Then, the instantaneous modal parameters can be identified by using the following estimator:

$$\begin{cases} \omega_{\mathrm{d}k}(t) = \dfrac{\mathrm{d}\varphi_k(t)}{\mathrm{d}t}, \\ \eta_k(t) = \dfrac{\mathrm{d}\left(\ln a_k(t)\right)}{\mathrm{d}t} \cdot \dfrac{1}{\omega_{\mathrm{d}k}(t)}, \\ \xi_k(t) = \sqrt{\dfrac{\eta_k(t)^2}{\eta_k(t)^2+1}}. \end{cases} \tag{21}$$

3.2. Energy Analysis Method for the Identification of Damping Ratio. As already noted, the higher precision of the identification of the IF can be obtained from the well-established TF representation, but for damping ratio identification based on amplitude envelope in equation (21), it has much lower identification accuracy since the amplitude envelope is easily disturbed by noise. In order to enhance the identification accuracy of the damping ratio, the estimator based on signal energy analysis for LTV systems is presented.

It can be assumed that the signal is time-invariant in a short time (that is, the frequency of the signal is not changed in a sampling period). For most signals without fast time-varying IF, this assumption can really be valid. Consider a time-varying signal as shown in Figure 2; the zero position of this signal is denoted as t_q, and the IF is considered to be constant within a sampling period T_q around t_q. In other words, the IF of the signal from time $t_q - T_q/2$ to time $t_q + T_q/2$ is denoted as $\omega_{\mathrm{d}k}(t_q)$. The signal energy of the first and second half sampling periods is calculated by E_{qu} and E_{qd}, respectively. They are given by

$$E_{\mathrm{qu}} = \int_{t_q-\left(T_q/2\right)}^{t_q} \ddot{x}_{pk}^2(t)\mathrm{d}t = A_{0k}^2 \int_{t_q-\left(T_q/2\right)}^{t_q} e^{-2\xi_k\left(t_q\right)\omega_{0k}\left(t_q\right)t} \cdot \cos^2\left(\omega_{\mathrm{d}k}\left(t_q\right)t + \varphi_{0k}\right)\mathrm{d}t, \tag{22}$$

$$E_{\mathrm{qd}} = \int_{t_q}^{t_q+\left(T_q/2\right)} \ddot{x}_{pk}^2(t)\mathrm{d}t = A_{0k}^2 \int_{t_q}^{t_q+\left(T_q/2\right)} e^{-2\xi_k\left(t_q\right)\omega_{0k}\left(t_q\right)t} \cdot \cos^2\left(\omega_{\mathrm{d}k}\left(t_q\right)t + \varphi_{0k}\right)\mathrm{d}t. \tag{23}$$

According to $\cos^2(\omega_{\mathrm{d}k}(t_q)t + \varphi_{0k}) = 1 - \sin^2(\omega_{\mathrm{d}k}(t_q)t + \varphi_{0k})$, equation (22) can be rewritten as

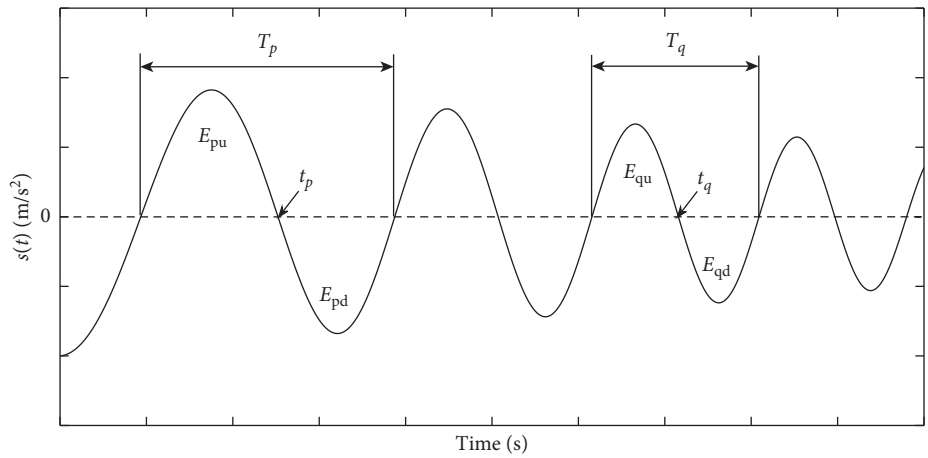

Figure 2: A time-varying signal for energy analysis.

$$E_{qu} = \frac{A_{0k}^2}{2}\int_{t_q-(T_q/2)}^{t_q} e^{-2\xi_k(t_q)\omega_{0k}(t_q)t}\mathrm{d}t + \frac{A_{0k}^2}{2}\int_{t_q-(T_q/2)}^{t_q} e^{-2\xi_k(t_q)\omega_{0k}(t_q)t}\cdot\cos 2\left(\omega_{dk}(t_q)t+\varphi_{0k}\right)\mathrm{d}t = \frac{A_{0k}^2}{2}\times B_1 + \frac{A_{0k}^2}{2}\times B_2, \tag{24}$$

where $B_1 = \int_{t_q-(T_q/2)}^{t_q} e^{-2\xi_k(t_q)\omega_{0k}(t_q)t}\mathrm{d}t$ and $B_2 = \int_{t_q-(T_q/2)}^{t_q} e^{-2\xi_k(t_q)\omega_{0k}(t_q)t}\cdot\cos 2(\omega_{dk}(t_q)t+\varphi_{0k})\mathrm{d}t$, which can be calculated by the real part of Γ_2:

$$\Gamma_2 = \int_{t_q-(T_q/2)}^{t_q} e^{-2\xi_k(t_q)\omega_{0k}(t_q)t}\cdot e^{j2(\omega_{dk}(t_q)t+\varphi_{0k})}\mathrm{d}t = \frac{e^{j2\varphi_{0k}}}{j2\omega_{dk}(t_q)-2\xi_k(t_q)\omega_{0k}(t_q)}\cdot\left[e^{(j2\omega_{dk}(t_q)-2\xi_k(t_q)\omega_{0k}(t_q))\cdot t_q} - e^{(j2\omega_{dk}(t_q)-2\xi_k(t_q)\omega_{0k}(t_q))\cdot(t_q-(T_q/2))}\right] = \frac{e^{j2\varphi_{0k}}\cdot\left[-j2\omega_{dk}(t_q)-2\xi_k(t_q)\omega_{0k}(t_q)\right]}{4\omega_{dk}^2(t_q)+4\xi_k^2(t_q)\omega_{0k}^2(t_q)}\cdot\left[e^{(j2\omega_{dk}(t_q)-2\xi_k(t_q)\omega_{0k}(t_q))\cdot t_q} - e^{(j2\omega_{dk}(t_q)-2\xi_k(t_q)\omega_{0k}(t_q))\cdot(t_q-(T_q/2))}\right]. \tag{25}$$

According to the inherent characteristics of the vibration system, the following conditions can be satisfied:

$$\omega_{dk}(t_q)T_q = 2\pi,\qquad \omega_{dk}(t_q) = \omega_{0k}(t_q)\sqrt{1-\xi_k^2(t_q)}. \tag{26}$$

Then, Γ_2 can be rewritten as

$$\Gamma_2 = \frac{e^{j2\varphi_{0k}}\cdot\left[-j2\omega_{dk}(t_q)-2\xi_k(t_q)\omega_{0k}(t_q)\right]}{4\omega_{0k}^2(t_q)}\cdot e^{(j2\omega_{dk}(t_q)-2\xi_k(t_q)\omega_{0k}(t_q))\cdot(t_q-(T_q/2))}\cdot\left[e^{(j2\omega_{dk}(t_q)-2\xi_k(t_q)\omega_{0k}(t_q))(T_q/2)}-1\right] = \frac{-j2\omega_{dk}(t_q)-2\xi_k(t_q)\omega_{0k}(t_q)}{4\omega_{0k}^2(t_q)}\cdot e^{j2\left[\omega_{dk}(t_q)(t_q-(T_q/2))+\varphi_{0k}\right]}\cdot e^{-2\xi_k(t_q)\omega_{0k}(t_q)\cdot(t_q-(T_q/2))}\cdot\left[e^{-2\pi\xi_k(t_q)/\sqrt{1-\xi_k^2(t_q)}}-1\right]. \tag{27}$$

In the same way, equation (23) can be rewritten as

$$E_{\mathrm{qd}} = \frac{A_{0k}^2}{2}\int_{t_q}^{t_q+\left(T_q/2\right)} e^{-2\xi_k\left(t_q\right)\omega_{0k}\left(t_q\right)t}\,\mathrm{d}t + \frac{A_{0k}^2}{2}\int_{t_q}^{t_q+\left(T_q/2\right)} e^{-2\xi_k\left(t_q\right)\omega_{0k}\left(t_q\right)t} \cdot \cos 2\left(\omega_{\mathrm{d}k}\left(t_q\right)t + \varphi_{0k}\right)\mathrm{d}t = \frac{A_{0k}^2}{2}\times B_3 + \frac{A_{0k}^2}{2}\times B_4, \tag{28}$$

where B_4 can be calculated by the real part of Γ_4:

$$\Gamma_4 = \frac{-j2\omega_{\mathrm{d}k}\left(t_q\right) - 2\xi_k\left(t_q\right)\omega_{0k}\left(t_q\right)}{4\omega_{0k}^2\left(t_q\right)} \cdot e^{j2\left[\omega_{\mathrm{d}k}\left(t_q\right)\left(t_q-\left(T_q/2\right)\right)+\varphi_{0k}\right]} \cdot e^{-2\xi_k\left(t_q\right)\omega_{0k}\left(t_q\right)\cdot t_q} \cdot \left[e^{-2\pi\xi_k\left(t_q\right)/\sqrt{1-\xi_k^2\left(t_q\right)}} - 1\right]. \tag{29}$$

From the above equations, the relationships can be obtained as follows:

$$\begin{cases} B_3 = e^{-\xi_k\left(t_q\right)\omega_{0k}\left(t_q\right)T_q}B_1, \\ B_4 = e^{-\xi_k\left(t_q\right)\omega_{0k}\left(t_q\right)T_q}B_2. \end{cases} \tag{30}$$

Therefore, when the IF has already been identified, the instantaneous damping ratio can be identified by the relationship between signal energy E_{qd} and signal energy E_{qd}:

$$\begin{cases} E_{\mathrm{qd}} = e^{-\xi_k\left(t_q\right)\omega_{0k}\left(t_q\right)T_q}E_{\mathrm{qu}}, \\ \xi_k\left(t_q\right) = -\ln\left(\dfrac{E_{\mathrm{qd}}}{E_{\mathrm{qu}}}\right)/\left(\omega_{0k}\left(t_q\right)T_q\right). \end{cases} \tag{31}$$

In such a way, the damping ratio $\xi_k(t_q)$ at each point t_q can be identified using the same method. Compared with the identification method based on amplitude envelope, the method based on energy analysis can effectively improve the robustness to noise.

4. Simulation Example

In order to validate the proposed method, a 3-DOF mass-spring-dashpot system with time-varying stiffness and time-varying damping is simulated as a numerical example. The LTV system is shown in Figure 3.

The initial parameters are given by

$$\begin{cases} m_1 = 0.5,\ m_2 = m_3 = 1\,(\mathrm{kg}), \\ k_1 = 8000, k_2 = 10000, k_3 = 6000, k_4 = 4000\,(\mathrm{N/m}), \\ c_1 = c_2 = 0.2, c_3 = c_4 = 0.3\ (\mathrm{Ns/m}). \end{cases} \tag{32}$$

The stiffness and damping variations for the case are given by

$$\begin{cases} \Delta k_1 = 12000\left\{\mathrm{atan}\left[10\times(-2)^2\right] - \mathrm{atan}\left[10\,(t-2)^2\right]\right\}, \\ \Delta k_3 = 1200\sin\left(1.5\pi t\right)\cdot t, \\ \Delta k_2 = \Delta k_4 = 0, \\ \Delta c_1 = \Delta c_2 = 0, \\ \Delta c_3 = -0.3\sin\left(0.8\pi t\right), \\ \Delta c_4 = 0.3t. \end{cases} \tag{33}$$

Assuming that an instantaneous impulse excitation is applied on the mass m_2 at the initial time, the Newmarkβ algorithm is used to compute the structural free response. The sampling time is 3 s, and the acceleration response data of the mass m_2 are shown in Figure 4. Then the identification method can be performed on the data.

To further validate the adaptiveness and improvement for the TF representation based on GLCT, the Morlet wavelet is selected as a TFA tool to extract the IF as a comparison. The TFA results are shown in Figures 5 and 6, respectively. It can be seen that the response signal contains three components. The IF of the first component varies slowly with time, and the IF of the other two components varies rapidly. For the TF representation around point (2 s, 20 Hz), instantaneous frequency trajectory based on GLCT is more clear and obvious and the TF representation based on GLCT has a higher resolution. However, at TF intervals (1−2 s, 15−25 Hz) and (1−3 s, 35−45 Hz), the Morlet wavelet appears to be inadequate for TF representation of these signal components with fast time-varying IF.

Therefore, the IF of the time-varying system can be identified by TF ridge extraction. The IF of each mode extracted by using the Morlet and GLCT are shown in Figures 7–9. Black lines in these figures are the theoretical values, and red dotted lines and blue dotted lines are the identified results by using GLCT and Morlet, respectively. The results clearly indicate that GLCT conduces to better performance in tracking fast time-varying IF than Morlet.

Once the IF of each mode is identified, the three time-varying components of the acceleration response can be exactly separated by the VK filter. The decomposition results are shown in Figure 10.

Moreover, the amplitude envelope of the three components is also computed, which can be used for the identification of the time-varying damping ratio. To further validate the robustness of the method based on energy analysis, the estimator based on signal amplitude in equation (21) is used to estimate the time-varying damping ratio as a comparison. The identified results are presented in Figures 11–13, and significant fluctuations are observed by using the estimator in equation (21). By comparison, the energy method based on half-period integral can effectively resist noise and get higher identification accuracy. Since the identification of the damping ratio is full of challenge and most modal identification methods are invalid for LTV systems, important

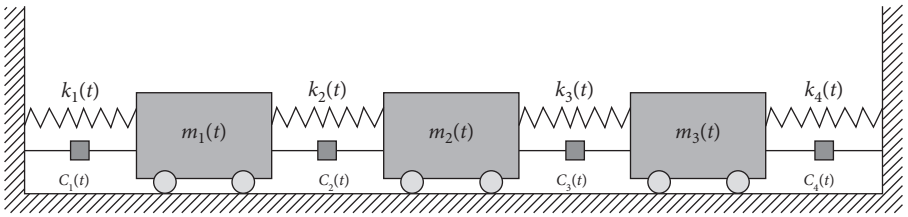

Figure 3: 3-DOF time-varying system.

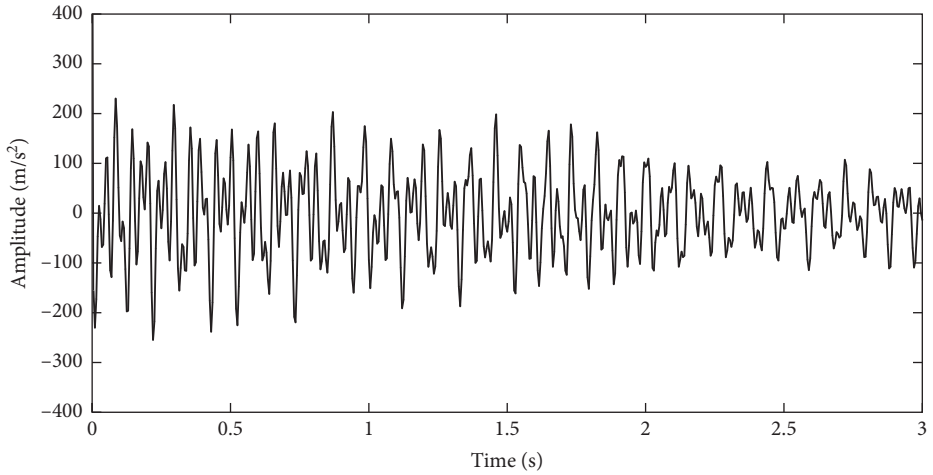

Figure 4: Acceleration response signal.

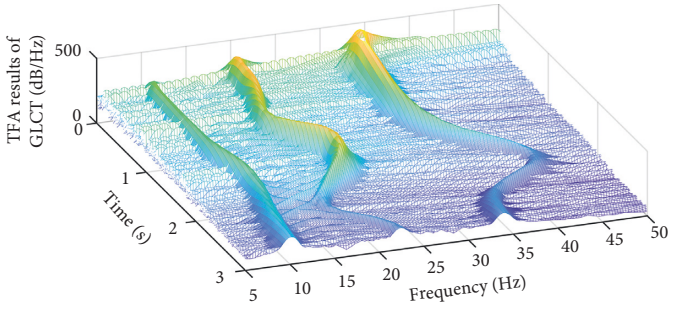

Figure 5: TFA results of GLCT.

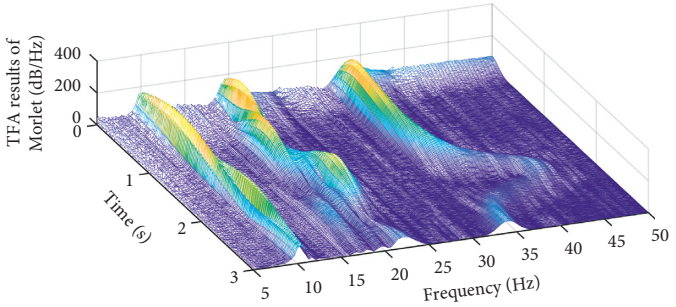

Figure 6: TFA results of the Morlet wavelet.

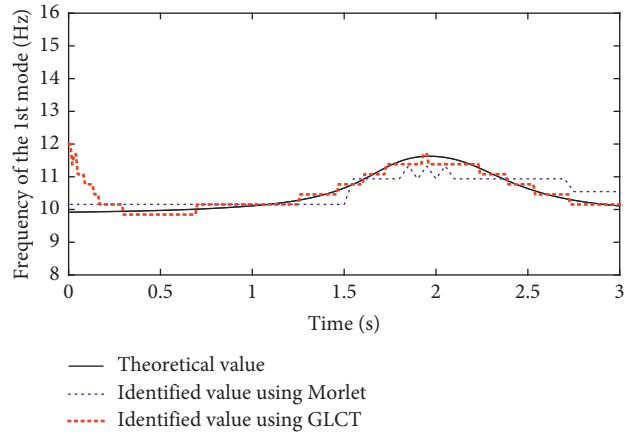

Figure 7: Theoretical results and identified results of the 1st mode.

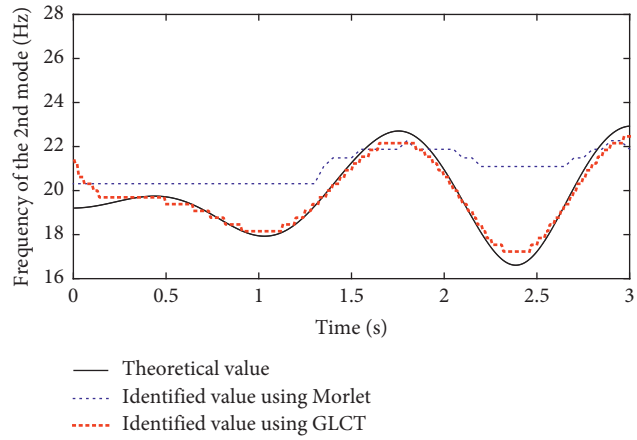

Figure 8: Theoretical results and identified results of the 2nd mode.

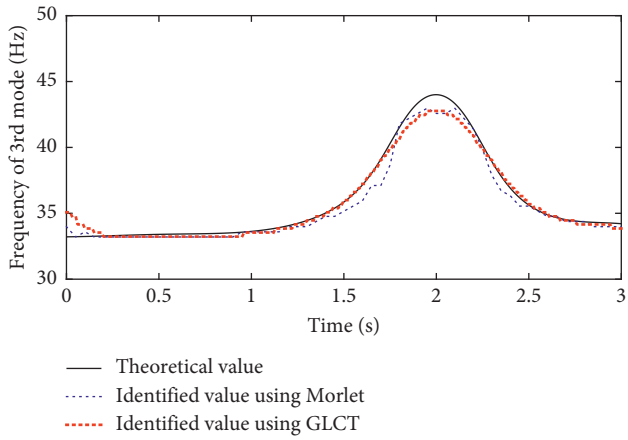

Figure 9: Theoretical results and identified results of the 3rd mode.

improvements have been made in instantaneous modal parameter identification by using energy analysis. In order to investigate the performance of the identification method, a root-mean-square error (RMSE) over the total sampling time is further computed to quantify the accuracy of identified results as

$$\mathrm{RMSE} = \sqrt{\frac{1}{N_s}\sum_{i=1}^{N_s}\left(\vartheta_i - \widetilde{\vartheta}_i\right)^2}, \tag{34}$$

where N_s represents the number of sampling points and ϑ_i and $\widetilde{\vartheta}_i$ represent the theoretical and identified instantaneous modal parameters, i.e., instantaneous frequencies and damping ratios, respectively. Therefore, the calculated RMSE values of instantaneous frequencies and damping ratios are listed in Table 2.

To further investigate the performance and reliability of the proposed method, different signal-to-noise ratios (SNR) of noise are added to the response of this structure. The same procedure as above is followed to identify the instantaneous modal parameters, and a mean absolute percentage error (MAPE) over the total sampling time is further computed to quantify the accuracy of the identified results as

$$\mathrm{MAPE} = \frac{1}{N_s}\sum_{i=1}^{N_s}\left|\frac{\vartheta_i - \widetilde{\vartheta}_i}{\vartheta_i}\right| \times 100\%, \tag{35}$$

where N_s represents the number of sampling points and ϑ_i and $\widetilde{\vartheta}_i$ represent the theoretical and identified instantaneous modal parameters.

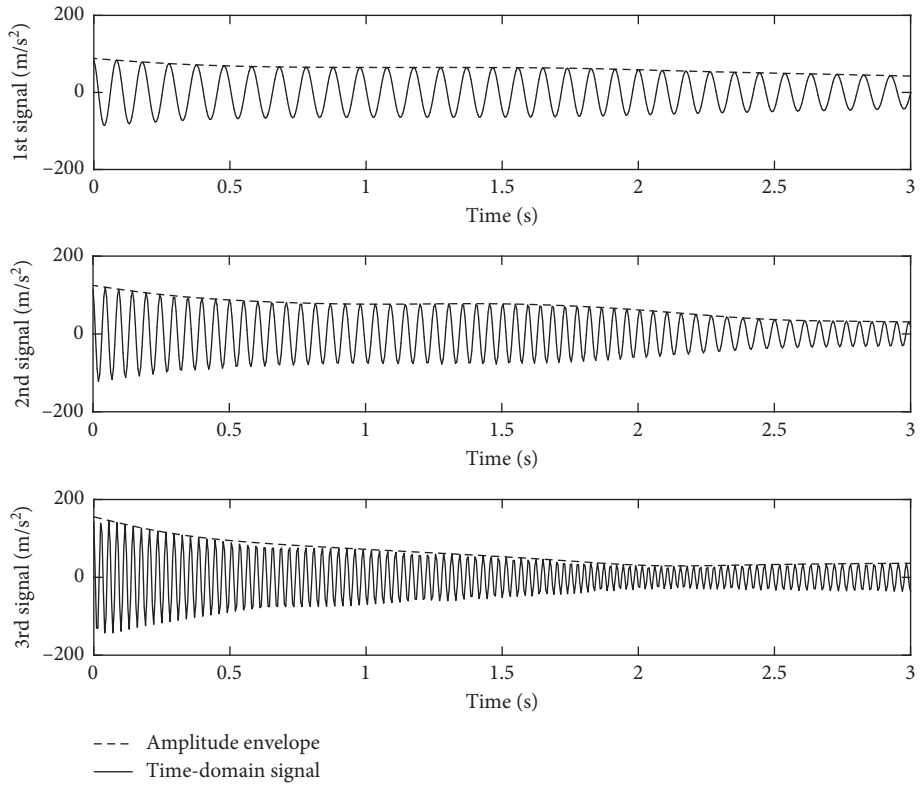

Figure 10: Amplitude envelope and component signal.

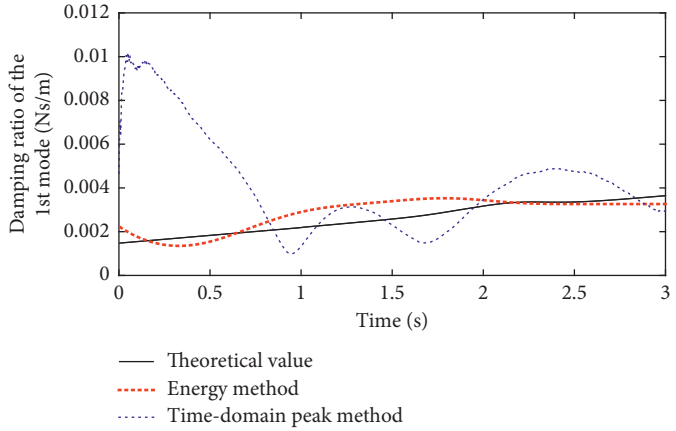

Figure 11: Theoretical results and identified results of the 1st mode.

Therefore, the calculated MAPE values under the effects of measurement noise are listed in Tables 3 and 4.

By comparing the RMSE values and MAPE values using different identification methods, it can be found that the proposed method has better performance in tracking time-varying parameters. The results also show the good adaptive ability and high accuracy even in low SNR scenarios. Especially for the identification of damping ratio, the energy analysis algorithm outperforms the traditional time-domain method.

For practical application of the proposed method, instantaneous frequencies and damping ratios can be identified only using one set of data from single-output. However, for the estimation of mode shapes of LTV systems, there are two hard issues in the implementation of this algorithm. Firstly, multiple sets of data from multioutput are needed to establish the mode shape matrix. Secondly, it is necessary to identify the time-varying mode shapes at each time point, which will lead to a large amount of calculation. Therefore, further studies should be done to estimate mode shapes and improve algorithm efficiency.

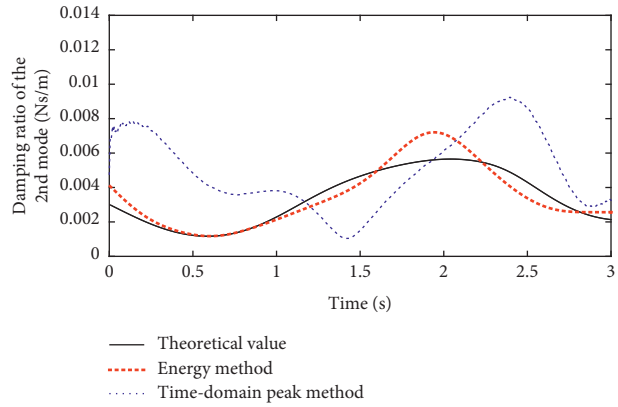

Figure 12: Theoretical results and identified results of the 2nd mode.

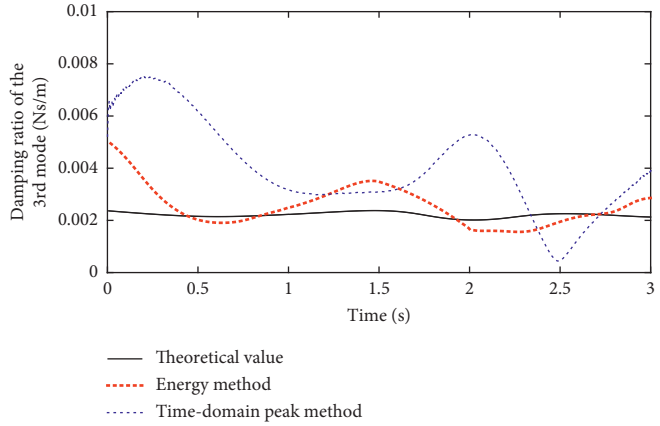

Figure 13: Theoretical results and identified results of the 3rd mode.

Table 2: Errors of identification results of instantaneous frequency.

RMSE	Mode	Morlet	GLCT
Instantaneous frequency	1st	0.306	0.195
	2nd	1.882	0.230
	3rd	0.599	0.331
RMSE	Mode	Time-domain algorithm	Energy algorithm
Instantaneous damping ratio	1st	3.006×10^{-3}	3.689×10^{-4}
	2nd	3.944×10^{-3}	8.792×10^{-4}
	3rd	2.511×10^{-3}	6.699×10^{-4}

Table 3: Errors of identification results of instantaneous frequency.

MAPE (%)	Mode	SNR (dB)			
		Noise-free	100	50	20
Morlet	1st	2.421	2.444	2.444	2.514
	2nd	8.141	8.152	8.153	8.157
	3rd	1.091	1.076	1.081	1.136
GLCT	1st	1.553	1.556	1.557	1.571
	2nd	1.305	1.312	1.314	1.316
	3rd	0.911	0.905	0.907	0.927

Table 4: Errors of identification results of the instantaneous damping ratio.

MAPE (%)	Mode	SNR (dB)			
		Noise-free	100	50	20
Time-domain algorithm	1st	>50	>80	>80	>100
	2nd	>50	>80	>80	>100
	3rd	>50	>80	>80	>100
Energy algorithm	1st	14.135	16.929	16.429	21.008
	2nd	20.873	21.560	21.607	21.396
	3rd	26.783	29.496	29.531	31.387

5. Conclusion

This paper proposes a method based on adaptive TF decomposition for instantaneous modal parameter identification of LTV systems. This method consists of two main steps. The first step is the IF extraction algorithm based on GLCT. By applying the algorithm to perform the VK filter, the free response of LTV systems can be decomposed into multiple mode responses. Then the other step is the energy analysis algorithm based on each mode response for the identification of the instantaneous damping ratio. Based on the results of numerical simulations, the corresponding conclusions can be concluded as following:

(1) GLCT is a more effective TFA tool than WT for the response signals of LTV systems. It can obtain the better TF representation with high energy concentration and therefore extract the IF with better accuracy.

(2) Since the wavelet transform is essentially a signal filter, application of a TFA tool with high energy concentration can enhance antinoise capability of parameter identification. By applying GLCT to perform the VK filter, it not only improves the adaptability of decomposition but also has good antinoise ability. It can be seen from the results of error analysis that our method has good immunity to noise.

(3) By adding different SNRs of noise, identification of the instantaneous damping ratio based on the time-domain algorithm and energy analysis algorithm is also discussed. The energy analysis algorithm can eliminate the influence of amplitude fluctuation in the time domain and improve the identification accuracy of the damping ratio. The results show that the energy analysis algorithm has better recognition accuracy, convergence, and noise immunity compared with the traditional method.

Data Availability

The raw data used to support the findings of this study have not been made available because the data also forms part of an ongoing study.

Conflicts of Interest

The authors declare that they have no conflicts of interest.

Acknowledgments

This work was funded by the National Natural Science Foundation of China (Grant nos. 11172131 and 11232007) and a Project Funded by the Priority Academic Program Development of Jiangsu Higher Education Institutions.

References

[1] R. Pintelon and J. Schoukens, *System Identification: A Frequency Domain Approach*, IEEE Press, Piscataway, NJ, USA, 2nd edition, 2001.

[2] S.-D. Zhou, L. Liu, W. Yang, and Z.-S. Ma, "Operational modal identification of time-varying structures via a vector multistage recursive approach in hybrid time and frequency domain," *Shock and Vibration*, vol. 2015, Article ID 397364, 13 pages, 2015.

[3] D.-Q. Li, S.-D. Zhou, L. Liu, J. Kang, and Y.-C. Ma, "A Bayesian estimator of operational modal parameters for linear time-varying mechanical systems based on functional series vector TAR model," *Journal of Sound and Vibration*, vol. 442, no. 3, pp. 384–413, 2019.

[4] K. Liu, "Extension of modal analysis to linear time-varying systems," *Journal of Sound and Vibration*, vol. 226, no. 1, pp. 149–167, 1999.

[5] Z. Y. Shi, S. S. Law, and H. N. Li, "Subspace-based identification of linear time-varying system," *AIAA Journal*, vol. 45, no. 8, pp. 2042–2050, 2007.

[6] I. Goethals, L. Mevel, A. Benveniste, and B. D. Moor, "Recursive output-only subspace identification for in-flight flutter monitoring," in *Proceedings of the 22nd International Modal Analysis Conference*, vol. 7, Dearborn, MI, USA, 2004.

[7] S. Pang, K.-P. Yu, and J. Zou, "Improved subspace method with application in linear time-varying structural modal parameter identification," *Chinese Journal Of Applied Mechanics*, vol. 22, no. 2, pp. 184–189, 2005.

[8] B. Zhou, X. Xie, X. Wang, R. Zhao, and Y.-H. Bai, "The Tunnel structural mode frequency characteristics identification and analysis based on a modified stochastic subspace identification method," *Shock and Vibration*, vol. 2018, Article ID 6595841, 12 pages, 2018.

[9] R. B. Mrad, S. D. Fassois, and J. A. Levitt, "A polynomial-algebraic method for non-stationary TARMA signal analysis—part I: the method," *Signal Processing*, vol. 65, no. 1, pp. 1–19, 1998.

[10] L. Ljung and S. Gunnarsson, "Adaptation and tracking in system identification—A survey," *Automatica*, vol. 1, no. 26, pp. 7–21, 1990.

[11] M. D. Spiridonakos and S. D. Fassois, "Adaptable functional series TARMA models for non-stationary signal modelling," *Ifac Proceedings Volumes*, vol. 45, no. 16, pp. 1276–1281, 2012.

[12] W. Yang, L. Liu, S.-D. Zhou, and Z.-S. Ma, "Modal parameter identification of linear time-varying structures using Kriging shape function," *Acta Aeronautica et Astronautica Sinica*, vol. 36, no. 4, pp. 1169–1176, 2015.

[13] Z.-Y. Shi, S. S. Law, and X. Xu, "Identification of linear time-varying MDOF dynamical systems from forced excitation using Hilbert transform and EMD method," *Journal of Sound and Vibration*, vol. 321, no. 3–5, pp. 572–589, 2009.

[14] R. Ghanem and F. Romeo, "A wavelet-based approach for the identification of linear time-varying dynamical systems," *Journal of Sound and Vibration*, vol. 234, no. 4, pp. 555–576, 2000.

[15] X. Xu, Z. Y. Shi, and Q. You, "Identification of linear time-varying systems using a wavelet-based state-space method," *Mechanical Systems and Signal Processing*, vol. 26, no. 1, pp. 91–103, 2012.

[16] Z. Hou, M. Noori, and R. S. Amand, "Wavelet-based approach for structural damage detection," *Journal of Engineering Mechanics*, vol. 126, no. 7, pp. 677–683, 2000.

[17] G. Zhang, B. Tang, and Z. Chen, "Operational modal parameter identification based on PCA-CWT," *Measurement*, vol. 139, pp. 334–345, 2019.

[18] K. Dziedziech, W. J. Staszewski, B. Basu, and T. Uhl, "Wavelet-based detection of abrupt changes in natural

frequencies of time-variant systems," *Mechanical Systems and Signal Processing*, vol. 64-65, pp. 347–359, 2015.

[19] Y. Xin, H. Hao, and J. Li, "Time-varying system identification by enhanced empirical wavelet transform based on synchroextracting transform," *Engineering Structures*, vol. 196, no. 1, Article ID 109313, 2019.

[20] A. Farzampour, A. Kamali-Asl, and J. W. Hu, "Unsupervised identification of arbitrarily-damped structures using time-scale independent component analysis: part I," *Journal of Mechanical Science and Technology*, vol. 32, no. 2, pp. 567–577, 2018.

[21] A. Farzampour, A. Kamali-Asl, and J. W. Hu, "Unsupervised identification of arbitrarily-damped structures using time-scale independent component analysis: part II," *Journal of Mechanical Science and Technology*, vol. 32, no. 9, pp. 4413–4422, 2018.

[22] I. Daubechies, J. Lu, and H.-T. Wu, "Synchrosqueezed wavelet transforms: an empirical mode decomposition-like tool," *Applied and Computational Harmonic Analysis*, vol. 30, no. 2, pp. 243–261, 2011.

[23] Y. Deng, C.-M. Cheng, Y. Yang, Z.-K. Peng, W.-X. Yang, and W.-M. Zhang, "Parametric identification of nonlinear vibration systems via polynomial chirplet transform," *Journal Of Vibration and Acoustics*, vol. 138, no. 5, p. 18, 2016.

[24] G. Yu and Y. Zhou, "General linear chirplet transform," *Mechanical Systems and Signal Processing*, vol. 70-71, pp. 958–973, 2015.

[25] K. S. Wang and P. S. Heyns, "Application of computed order tracking, Vold-Kalman filtering and EMD in rotating machine vibration," *Mechanical Systems and Signal Processing*, vol. 25, no. 1, pp. 416–430, 2011.

[26] Y.-F. Yang, S. Li, and H.-L. Li, "Improved ITD method for structural modal parameter identification under ambient excitation," *Journal Of Vibration and Shock*, vol. 33, no. 1, pp. 194–199, 2014.

[27] Z.-P. Weng and Y.-N. Xi, "Application of correlation analysis in structural damping ratio measurement using time-domain attenuation method," *Journal Of Ship Mechanics*, vol. 13, no. 4, pp. 657–661, 2009.

[28] R. J. Marceau and S. Soumare, "A unified approach for estimating transient and long-term stability transfer limits," *IEEE Transactions on Power Systems*, vol. 14, no. 2, pp. 693–701, 1999.

[29] D. Bernal, "Kalman filter damage detection in the presence of changing process and measurement noise," *Mechanical Systems and Signal Processing*, vol. 39, no. 1-2, pp. 361–371, 2013.

[30] H. Vold, H. Herlufsen, and M. Mains, "Multi axle order tracking with the Vold-Kalman tracking filter," *Journal of Sound and Vibration*, vol. 13, no. 5, pp. 30–34, 1997.

[31] A. Bagheri, O. E. Ozbulut, and D. K. Harris, "Structural system identification based on variational mode decomposition," *Journal of Sound and Vibration*, vol. 417, pp. 182–197, 2018.